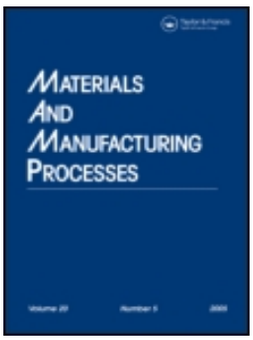

Materials and Manufacturing Processes

ISSN: 1042-6914 (Print) 1532-2475 (Online) Journal homepage: https://www.tandfonline.com/loi/lmmp20

Composition Modulated Multilayer Zn–Fe Alloy Coatings on Mild Steel for Better Corrosion Resistance

K. Venkatakrishna & A. Chitharanjan Hegde

To cite this article: K. Venkatakrishna & A. Chitharanjan Hegde (2011) Composition Modulated Multilayer Zn–Fe Alloy Coatings on Mild Steel for Better Corrosion Resistance, Materials and Manufacturing Processes, 26:1, 29-36, DOI: 10.1080/10426914.2010.501192

To link to this article: https://doi.org/10.1080/10426914.2010.501192

Published online: 03 Mar 2011.

Submit your article to this journal

Article views: 495

View related articles

Citing articles: 1 View citing articles

Full Terms & Conditions of access and use can be found at
https://www.tandfonline.com/action/journalInformation?journalCode=lmmp20

Materials and Manufacturing Processes, 26: 29–36, 2011
Copyright © Taylor & Francis Group, LLC
ISSN: 1042-6914 print/1532-2475 online
DOI: 10.1080/10426914.2010.501192

Taylor & Francis
Taylor & Francis Group

Composition Modulated Multilayer Zn–Fe Alloy Coatings on Mild Steel for Better Corrosion Resistance

K. Venkatakrishna and A. Chitharanjan Hegde

Electrochemistry Laboratory, Department of Chemistry, National Institute of Technology Karnataka, Srinivasnagar, India

Composition modulated alloy (CMA) of Zn–Fe coatings were developed on mild steel galvanostatically from chloride bath containing sulphanilic acid (SA) and ascorbic acid (AA) through single bath technique (SBT). The properties of CMA coatings were found to depend on the thickness of individual layers and switching cathode current densities (SCCDs). The CMA (Zn–Fe) coating, having 120 layers, deposited at 20 and 50 mA cm^{-2}, were found to show the least corrosion rate (1.545×10^{-2} mmy^{-1}) compared to monolithic alloy (32.5×10^{-2} mmy^{-1}) of the same thickness. The improved corrosion resistance of multilayered coatings was due to the fact that the defects and failures occurring in a single layer in the deposition process is covered by the successively deposited coating layers, and hence the corrosive agent path is extended or blocked. Further, the high corrosion resistance of CMA Zn–Fe coatings was attributed to the "dielectric barrier" of the coatings, evidenced by dielectric spectroscopy and Mott–Schottky's plot. The corrosion rate was found to increase at high degree of layering, and is attributed to less relaxation time for redistribution of metal ions in diffusion layer, during plating. In other words, at higher layer thickness, the CMA coating tends to become a monolithic. CMA coatings were characterized by scanning electron microscopy (SEM) and atomic force microscopy (AFM).

Keywords AFM; Composition modulated multilayer alloy; Corrosion mechanism; Electrodeposition; Optimization; SEM study; Switching cathode current density; Zn–Fe coatings.

Introduction

In the past decades, several attempts have been made to develop highly corrosion resistant coatings. The development of Zn-based alloys has been of much interest for the protection of steel substrates [1]. Commonly electrodeposited alloy coatings consist of Zn–M (where M=Ni, Co, Fe, and Mn) [2–4]. Amongst them, Zn–Ni alloy has been studied extensively and put into practical uses in the mass production of steel sheets for automobile bodies and also for small components such as nuts and bolts [1–3]. Despite the fact that the development of Zn–Ni alloy coatings has produced a larger improvement in the corrosion resistance than that of the pure zinc coatings, further development for getting even better protective properties is of distinct commercial interest. Possibly, a relatively new electrodeposited coating called composition modulated multilayer (CMM) coatings is a possible further route to enhance the efficacy of simple monolithic Zn–Ni alloy coatings [5]. CMM coatings consist of a large number of thin alternate metal layers or alloy layers, and each layer plays its own distinctive role in achieving preferred performances. The development of zinc-based CMM coatings for the protection of steel substrates has been investigated recently [6–8]. Zinc and nickel CMM coatings electrodeposited from dual baths showed enhanced anti-corrosion performance. Kirilova et al. reported the anodic behavior of composition modulated Zn–Co multilayer electrodeposited from single and dual baths [9]. The coatings were developed under different conditions of current density, and their anodic behaviors were studied. CMM coatings obtained from dual baths dissolve at potentials that are close to those for pure Co coatings. CMM coatings obtained from a single bath dissolve at potentials between the dissolution potentials of pure Co and pure Zn coatings.

Zinc and Zn–Ni alloy CMM coatings were electrodeposited on to a steel substrate by the successive deposition of zinc and Zn–Ni alloy sublayers from dual baths [10]. The coated samples were evaluated in terms of the surface appearance, surface and cross-sectional morphologies, as well as corrosion resistance. The layered structure and the existence of microcracks caused by the internal stress in the thick Zn–Ni alloy sub layers were observed. CMM coatings were found to be more corrosion-resistant than the monolithic coatings of zinc or Zn–Ni alloy of same thickness. The possible reasons for the better protective performance of Zn–Ni/Zn CMM coatings were given on the basis of the analysis on the micrographic features of zinc and Zn–Ni alloy. A probable corrosion mechanism of zinc and Zn–Ni alloy CMM coatings was also proposed. The zinc sublayers beneath the Zn–Ni alloy top layer dissolves through the pores and microcracks existing in the Zn–Ni alloy deposits existing during corrosion. As a whole, the protection efficacy of Zn/Zn–Ni coatings was explained by the barrier effect of the Zn–Ni alloy sublayers and the sacrificial effect of the zinc sublayers. Varieties of zinc and Zn–Co alloy CMM coatings were electrodeposited onto steel substrates using dual bath technique [11]. The experimental results showed that the zinc and Zn–Co alloy CMM coatings were more

Received March 15, 2010; Accepted June 9, 2010

Address correspondence to A. Chitharanjan Hegde, Electrochemistry Laboratory, Department of Chemistry, National Institute of Technology Karnataka, Srinivasnagar 575 025, India; E-mail: achegde@rediffmail.com

corrosion-resistant than corresponding monolithic coatings of same thickness. The application of zinc and zinc alloy-based systems was reviewed by Wilcox [12]. The concept of production of CMM coatings, concentrating on their application as protective coatings for metal surfaces was examined. Zn–Ni, Zn–Fe, Zn–Co, and Zn–Mn alloys have been reported to be electrodeposited in multilayer format. Electrodeposition methods, bath chemistries, and coating morphologies and performances in appropriate corrosion tests were also reviewed.

Most of the work reported above explains the development of CMM Zn-based alloys using double bath technique (DBT), in which successive layers of alternating composition was obtained from two separate electrolytes having either pure Zn^{+2} and M^{+2} (where M=Ni, Co, and Fe) ions or Zn^{+2} and $(Zn^{+2} + M^{+2})$ ions. The deposition conditions were optimized, and results were discussed. The coating behaviors were assessed either by their dissolution potentials or by E_{corr} values, without determining their corrosion rates. In this direction, optimization of an acid chloride bath for production of CMM Zn–Co alloy showing peak performance against corrosion, using SBT was reported by Thangaraj et al. [13]. Though among CMM Zn-based alloy baths, Zn–Fe is very cheap it is less investigated, because of its instability, associated with oxidation of Fe^{+2} to Fe^{+3}, and also due to less corrosion resistance (compared to Zn–Ni and Zn–Co). In this work it is attempted to develop a stable bath having sulphanilic acid (SA) as brightener and ascorbic acid (AA) as antioxidant. The deposition conditions were optimized for peak performance of the coatings against corrosion. The corrosion rates were calculated from Tafel's extrapolation method, and were supported by electrochemical impedance spectroscopy (EIS) study. The role of SA in modulation of the alloy composition was tried to identify by cyclic voltammetry (CV) study. The article reports the optimization of bath conditions and operating parameters for development of CMA coating of Zn–Fe and its characterization, concentrating on their application as protective coatings for metal surfaces.

Experimental details

The initial studies focused on optimization of an electrolytic bath through standard Hull cell method. Monolithic Zn–Fe alloy deposits were developed at different current densities from the optimized bath containing $50\,g\,cm^{-3}$ $ZnCl_2$, $10\,g\,cm^{-3}$ $FeCl_2$, $50\,g\,cm^{-3}$ KCl, $140\,g\,cm^{-3}$ NH_4Cl, $5\,g\,cm^{-3}$ gelatin, $1\,g\,cm^{-3}$ SA, and $10\,g\,cm^{-3}$ AA. The electrolyte having Zn^{+2} and Fe^{+2} ions was prepared using LR grade chemicals and distilled water. Zn–Fe CMA deposition was carried out by SBT from optimized bath. Prepolished mild steel panels with active surface area of $2.5 \times 3.0\,cm^2$ were used as cathode and pure zinc as anode. Depositions were carried out galvanostatically in a constantly stirred electrolyte maintained at pH 3.5 and temperature 30°C. All deposition were carried out using high precision power source, AGILENT, N6705A, and their characterization were made using potentiostat/galvanostat (VersaSTAT3, Princeton Research).

The periodic change in the current density allows the growth of layers on substrate with alternate chemical compositions. That is, pulses of low current density results in layers of low Fe content, and pulses of high current density results in layers of high Fe content. The instrument was set to produce two different cathode current densities, called switching cathode current densities (SCCDs) in repetitive way. The thickness of the each layer was controlled by the duration of each current pulse and total number of layers was fixed by adjusting time for each cycle. Thus, CMA coatings of different configurations were produced. Such multilayer coatings are hereafter represented as $(Zn–Fe)_{1/2/n}$, where (Zn–Fe) represents alloy of Zn and Fe, and 1 and 2 represent cathode current density that cycles, and 'n' represents the total number of layers formed during total deposition time (10 min).

The corrosion study was carried out in a three-electrode system corrosion cell (250 ml), at 25°C in 5% NaCl solution at pH 6.0, prepared in distilled water. Polarization studies were performed at a scan rate of $1.0\,mV\,s^{-1}$ in a potential ramp of +0.5 V cathodic and −1.0 V anodic from open circuit potential (OCP). Saturated calomel electrode (SCE) was used as reference electrode and platinum as counter electrode. The impedance behavior of Zn–Fe alloy deposits was studied by drawing the Nyquist plot in the frequency range from 100 kHz to 10 mHz, using 10 mV perturbing voltage. The composition of coatings was analyzed by colorimetric method by stripping the electrodeposits into dilute HCl. The surface morphology and the surface roughness were measured by atomic force microscopy (AFM) (PicoSPM™ from Molecular Imaging). The microstructure confirming the layer formation was analyzed by scanning electron microscopy (SEM) (Model JSM-6380 LA from JEOL Japan). The mechanism of corrosion was identified by cyclic polarization study.

Results and discussion

Bath Chemistry

It was observed that addition of SA improved the brightness and uniformity of coatings. Fourier transform infrared (FTIR) spectroscopy revealed the presence of S–O and N–H groups in the coating. The SA may act as a brightener and as a complexing agent in present system. Gelatin was added (as primary additive) to electroplating baths (e.g., in zinc electrodeposition) to control the deposition rate, crystallization, leveling, and brightness of the deposit. Due to its very high molecular weight, its content in the plating baths in the present study represents concentrations, which were several orders of magnitude smaller than the concentrations of the zinc and iron ions. Thus, gelatin could not act as a complexing agent.

The deposition potential of Zn–Fe system, without additives was approximately −1.08 V. as shown in Fig. 1. In the anodic sweep, the Zn–Fe system shows the two peaks: at −0.95 (may be related to pure Zn), and −0.58 V (may be related either pure Fe or to a Zn–Fe phase). When SA was added, the deposition potential was unaltered. The oxidation peaks slightly shifted to −0.92 and −0.59 V. While the area below the first oxidation peak (charge) increased, that below the second oxidation peak decreased. The presence of gelatin in the bath apparently changed the shape of the voltammogram significantly. The deposition started

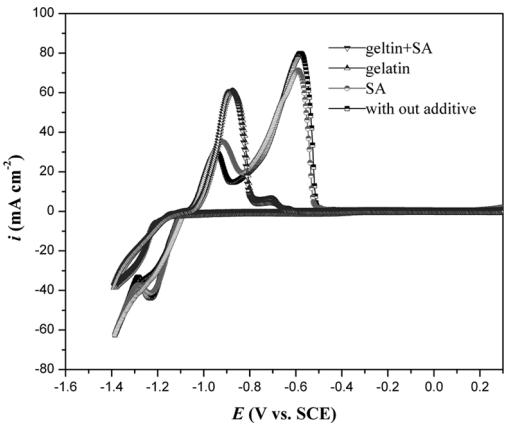

FIGURE 1.—Cyclic voltammograms for Zn–Fe, baths demonstrating the effect of gelatin and SA. Working electrode: Pt, pH = 3.5, $T = 30°C$, $\upsilon = 10\,mVs^{-1}$.

at −1.14 V and the deposition current density decreased. In the anodic sweep, the first oxidation peak shifted to −0.87 V and the associated charge increased. The second oxidation peak, on the other hand, became a shoulder with significantly reduced intensity and shifted to −0.68 V. When both gelatin and SA were present in the bath, gelatin apparently dictated the shape of voltammogram, namely, the deposition potential and the oxidation peaks were same.

Monolithic Zn–Fe Coating

Acid bath containing $ZnCl_2$, $FeCl_2$, SA, AA, and gelatin has been optimized by conventional Hull cell method at 1 A cell current, pH 3.5, and temperature 30°C. Varieties of deposits having grayish white/bright/semi-bright/porous/black powdery appearance were obtained over wide range of current density, 10–50 mA cm^{-2}. Effect of each bath constituents on Hull cell panels were examined in terms of their appearance, brightness, and surface morphology. NH_4Cl and KCl were used as complexing and conducting salts for improving the homogeneity and brightness of the deposit. AA was used to prevent the oxidation of Fe^{+2} to Fe^{+3} in the electrolytic bath. Bright uniform monolithic Zn–Fe alloy deposit with Fe content of 3.16% was produced at current density of 30 mA cm^{-2}, showing corrosion rate 32.5×10^{-2} mmy^{-1}. Zn–Fe alloy with 2.18 and 4.99 % of Fe content was obtained at 20 and 50 mA cm^{-2}, respectively. The corresponding corrosion rates were found to be 38.0×10^{-2} and 50.2×10^{-2} mmy^{-1}, respectively, (Table 2).

Zn–Fe CMA Coating

It was shown that TiAlN/AlN multilayer coatings produced by physical vapor deposition (PVD) process offers better thermo/mechanical properties than monolayered coatings in cutting tool applications [14]. The microstructure and growth morphologies depend on sputtering conditions. Composition, texture, and grain size of deposited coatings are highly dependent on the deposition conditions. The corrosion resistance of the substrate can thus be greatly improved by proper alloying [15]. Electrodepositon of CMM Zn–Ni coating from single acidic bath by potentiostatic method was reported by Prabhu Ganesan and et al. [16]. It was found that the Ni content varied as a function of thickness by applying a varying potential sequence. It was concluded that at higher potentials γ-phase corresponding to (600) planes are preferentially deposited while lower potentials leads to the deposition of other crystal planes of γ-phases (222), (330), and (444). With this incentive, it has been attempted to bring modulation in CMA Zn–Fe coatings. A precise control of the SCCDs allows the production of alternate layers of Zn–Fe with different composition and, consequently, different properties. The most important requirement for the CMA materials to exhibit improved property is a clear demarcation between layers without interlayer diffusion. To achieve this, SCCDs should be properly selected before to go for a high degree of layering. Hence, few sets of SCCDs have been selected arbitrarily (based on the nature of monolithic alloy coating) and CMA coatings have been developed. By fixing some number of layers (say, 20 layers), CMA coatings with different configuration were developed, and their corrosion rates were measured; they are reported in Table 1. This procedure allowed the selection of proper SCCDs at which the coating is most resistant to corrosion.

Optimization of Switching Cathode Current Densities (SCCDs). CMA deposits having 20 layers have been developed at different sets of SCCD's from 10–50 mA cm^{-2}. Table 1 demonstrates the effect of SCCDs (with varying difference between two current densities) on the corrosion behavior of Zn–Fe CMA coatings. The lowest corrosion rate was measured in case of $(Zn–Fe)_{20/50}$, with 30 mA cm^{-2} difference between two cathode current density. This large difference between SCCDs allowed the growth of two layers with large modulation in composition. This set of current densities was selected for further study of effects of the number of layers as described in the following subsection.

Optimization of Overall Number of Layers. The properties of CMA electrodeposits, including their corrosion resistance, may often be improved by increasing the total

TABLE 1.—Effect of SCCDs on corrosion properties of Zn–Fe CMA coatings obtained with 20 layers.

$(Zn–Fe)_1/(Zn–Fe)_2$ coatings with difference between SCCDs	SCCD mA cm^{-2}	E_{corr} (Volts)	i_{corr} (μA cm^{-2})	Corrosion rate $\times 10^{-2}$ mmy^{-1}
10 mA cm^{-2}	10–20	−1.108	12.64	18.24
	20–30	−1.048	4.21	6.076
	30–40	−1.107	8.21	11.84
	40–50	−1.104	13.65	19.70
15 mA cm^{-2}	10–25	−1.051	6.38	9.21
	20–35	−0.944	3.09	4.46
	30–45	−0.991	4.93	7.11
	40–55	−1.045	2.85	4.11
20 mA cm^{-2}	10–30	−1.111	9.48	13.67
	20–40	−1.23	3.53	5.09
	30–50	−1.087	2.09	3.01
30 mA cm^{-2}	10–40	−1.062	3.01	4.34
	20–50	−0.985	1.93	2.78

TABLE 2.—Comparison of corrosion parameters of monolithic Zn–Fe alloy and CMA Zn–Fe coatings at different current density and effect of number of layers on corrosion rate at 20–50 mA cm^{-2} (optimized SCCDs).

Configuration	No. of layers	E_{corr} (Volts)	i_{corr} (μA cm^{-2})	Corrosion rate $\times 10^{-2}$ mmy^{-1}
$(Zn–Fe)_{20}$ mA cm^{-2}	Monolithic	−1.164	26.39	38.0
$(Zn–Fe)_{30}$ mA cm^{-2}		−1.144	22.58	32.5
$(Zn–Fe)_{50}$ mA cm^{-2}		−1.127	34.88	50.2
$(Zn–Fe)_{20/50}$ mA cm^{-2}	4	−1.107	13.311	19.20
	6	−0.995	3.349	4.832
	10	−0.966	2.078	2.994
	20	−0.985	1.934	2.789
	60	−1.049	1.678	2.420
	120	−1.033	1.071	1.545
	300	−1.029	4.134	5.243
	600	−1.108	12.48	18.78

number of layers (usually, up to an optimal number), as long as the adhesion between layers is not deteriorated. Therefore, at the optimal combination of SCCD (20–50 mA cm^{-2}), CMA coatings with 20, 60, 120, 300, and 600 layers were produced including 4, 6, 10 layers. As evident from Table 2, the corrosion rate decreased substantially with increase in number of layers only up to 120 layers, and then decreased.

The decrease of corrosion rate at high degree of layering is attributed to less relaxation time for redistribution of solutes in the diffusion layer, during plating [17]. As the number of layers increased, the time for the deposition of each layer, say, $(Zn–Fe)_1$ is small (as the total time for deposition remains same). At high degree of layering, there is no sufficient time for metal ions to relax (against diffusion under given current density) and to get deposit on cathode with different composition. As a result, at high degree of layering modulation in composition is not likely to take place. In other words, CMA deposit is tending towards monolithic, showing less corrosion resistance. The least corrosion rate (1.545×10^{-2} mmy^{-1}) was observed for a coating with 120 layers (Table 2). Therefore, coating represented by, CMA $(Zn–Fe)_{20/50/120}$ was considered as the optimum configuration, with superior corrosion resistance.

While the total thickness of the coating was estimated by Faraday's law, it was verified by measurements, using a digital thickness meter (Coat measure model M & C). Then, the thickness of each layer in CMA coating having $(Zn–Fe)_{20/50/120}$ configuration was calculated from the total thickness (10 μm under given condition) and number of layers allowed to form (120). It was found that the thickness of each layer is about 85 nm.

Potentiodynamic Polarization Study. Figure 2 shows the potentiodynamic polarization curves of CMA Zn–Fe coatings with different number of layers. Tafel's extrapolation on such curves resulted in determination of the corrosion potential, corrosion current density, and corrosion rate, as listed in Table 2. As mentioned before, the increase of the number of layers resulted in a decrease in the corrosion rate. It is evident from Fig. 2 that the increase in the number of layers results in the increase of the barrier properties of

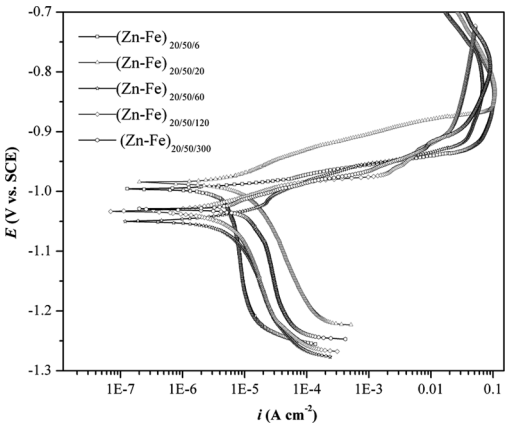

FIGURE 2.—Comparison of polarization behavior of CMA $(Zn–Fe)_{20/50}$ coating system with different number layers.

the coatings up to 120 layers and then in decrease, which is evident from the less i_{corr} values, as reported.

EIS is a suitable technique to gain valuable information on the capacitive behavior of the coating, responsible for improved corrosion resistance. Information about the interaction of coating with corrosion medium is obtained from Nyquist plots. It may be observed that in $(Zn–Fe)_{20/50}$ coating systems, the radius of the semicircle increased with number of layers only up to 120 layers as shown in Fig. 3 (only representative plots are given). It may be noted that the solution resistance R_s is nearly identical in all cases, as the same bath chemistry and cell configuration were used. The increase of polarization resistance R_P with increase in number of layers shows its improved corrosion resistance. It was found that at higher degree layering, such as 300 layers, the radius of the semicircle decreased drastically, indicating its poor corrosion protective performance.

Cyclic polarization study was carried out to understand the mechanism of corrosion. The polarization curve shown in Fig. 4 (arrow marks show the direction of scan) indicates that initiation and propagation of localized corrosion occurs at corrosion potentials of Zn–Fe CMA coating. The potential is swept in a single cycle, and the size of the hysteresis is

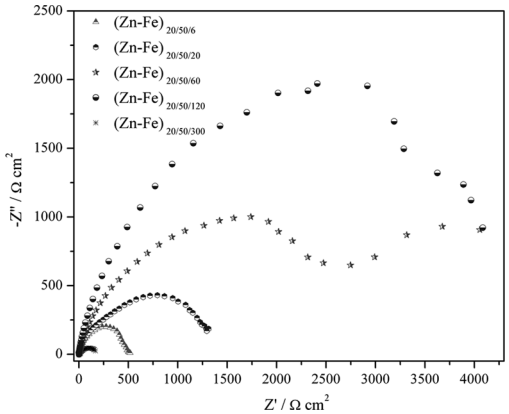

FIGURE 3.—Comparison Nyquist responses of CMA $(Zn–Fe)_{20/50}$ coating system with different number layers.

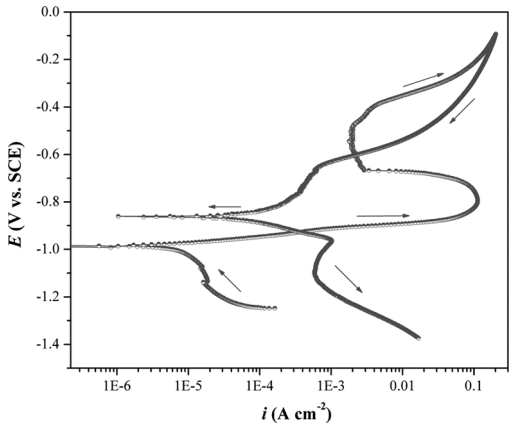

FIGURE 4.—Cyclic polarization behavior of CMA $(Zn–Fe)_{20/50/20}$ coating system at scan rate $1.0\,mV\,s^{-1}$).

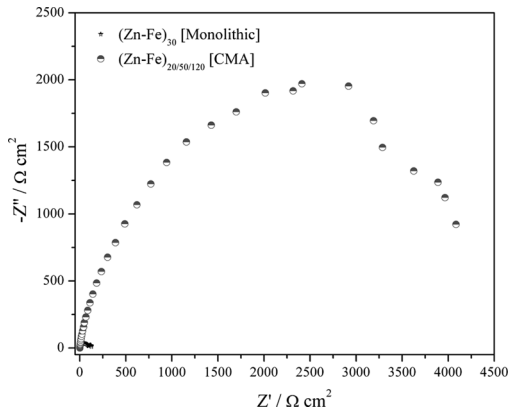

FIGURE 6.—Impedance resposnce of monolithic Zn–Fe and CMA $(Zn–Fe)_{20/50/120}$ coating systems deposited under optimal conditions of the bath.

examined along with the differences between the values of the starting open circuit corrosion potential and the return passivation potential. The existence of the hysteresis is indicative of pitting, while the size of the loop is related to the amount of pitting.

Comparison between the Corrosion Behavior of Monolithic and CMA Zn–Fe Coatings

On comparing the values given in Table 2, it becomes apparent that the corrosion rate of the CMA coating with $(Zn–Fe)_{20/50/120}$ configuration is ~20 times lower than that of the monolithic Zn–Fe coating, with same thickness. Relative polarization behavior of monolithic and multilayer Zn–Fe coatings (both under optimal conditions) is shown in Fig. 5. It may be observed that CMA coating with 120 layers reports least i_{corr} value. Similarly, the Nyquist response of monolithic and multilayer coatings of Zn–Fe alloy is shown comparatively in Fig. 6. It may be noted that large capacitive loop, corresponding to $(Zn–Fe)_{20/50/120}$ is indicative of its high corrosion resistance, with respect to that of monolithic alloy.

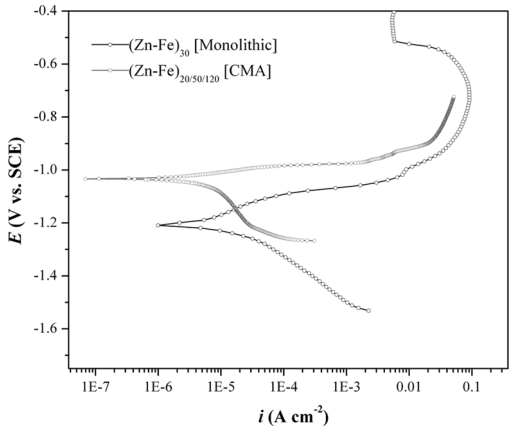

FIGURE 5.—Polarization behavior of monolithic Zn–Fe and CMA $(Zn–Fe)_{20/50/120}$ coating systems deposited under optimal conditions of the bath.

The experimental results showed that the corrosion rate of CMA Zn–Fe coatings developed under optimal conditions is more (1.54×10^{-2} mmy^{-1}) compared to that of CMA Zn–Ni alloy coatings (0.50×10^{-2} mmy^{-1}), reported by Prabhu Genesan et al. [16]. This is due to the genuine reason of Ni, which is nobler than Fe. The improved corrosion resistance of multilayer coatings is due to small change in the wt% Fe in alternate layers. The variation in composition brings a significant change in the phase structure of alloys as discussed earlier. Defects and failures occurring in a single layer in the deposition process are covered by the successively deposited coating layers. Therefore, the corrosive agent path is extended or blocked.

Dielectric Barrier of Coatings

EIS data points can also be used to study the dielectric properties of materials, and the technique is called dielectric spectroscopy. It is based on the interaction of an external field with the electric dipole moment of the sample, often expressed by permittivity. This technique measures the relative dielectric constant of a system over a range of frequencies, and the frequency response of the system, including the energy storage and dissipation properties can be identified.

In the presence of a material having dielectric constant ε_M, the surface charge density on the plates of a capacitor may be represented by [18]

$$\sigma = \varepsilon_M E + P \tag{1}$$

where σ is the surface charge density (quantity of charge per unit area of capacitor plate, C/m^2) is proportional to the electric field (E) and polarization (P). The value of σ for a medium is more than that for a vacuum, due to presence of the dielectrics of the medium. For many dielectric materials, P is proportional to E through the relationship

$$P = \varepsilon_0(\varepsilon_r - 1)E \tag{2}$$

where ε_0 is the dielectric constant of vacuum, and ε_r is the relative dielectric constant of the medium. The

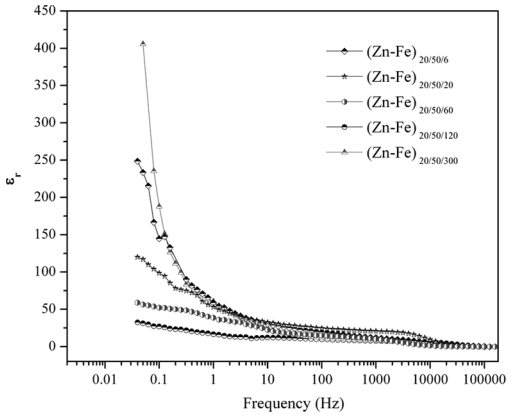

FIGURE 7.—Frequency response of relative dielectric constant ε_r of CMA $(Zn–Fe)_{20/50}$ coating system having different number layers.

variation of ε_r with frequency (from 10 mHz to 100 kHz) for different coating system $(Zn–Fe)_{20/50/6}$, $(Zn–Fe)_{20/50/20}$, $(Zn–Fe)_{20/50/60}$, $(Zn–Fe)_{20/50/120}$, and $(Zn–Fe)_{20/50/300}$ is shown in Fig. 7. It may be observed that ε_r is dependent to the frequency at lower limit, and almost independent of it at higher limit. It is due to the fact that, at high frequencies, there is no charging of the capacitor and the capacitance is effectively like that of an open circuit (vacuum). Hence, ε_r is almost same irrespective of the number of layers. At low frequency, the capacitor will be charged, and the capacitance is effectively like that of a closed circuit [19, 20]. Under this condition, the capacitance of electrical double layer (EDL) depends on the value of ε_r. It may be observed that the value of ε_r for CMA $(Zn–Fe)_{20/50/120}$ coating system is small compared to that of other coating systems, as shown in Fig. 7. In case of coatings showing high ε_r, the space charge density is very large (Eq. 2), and charge carriers have to flow from the positive to the negative plate to reestablish the voltage. But, in case of $(Zn–Fe)_{20/50/120}$, the space charge density is very small, and hence no much charge carriers are involved. Therefore, it may be inferred that the improved corrosion resistance of CMA Zn–Fe alloy coatings is due to impeded movement of charge carriers at the interface, caused by layers (suitable) of different dielectric properties.

Mott–Schottky Study

The semiconductor property of the coatings is responsible for its improved corrosion resistance and is due to impeded movement of charge carriers in the medium. The relationship between the type of semiconductor and the charge carriers involved is given by the Mott–Schottky equation [21]:

$$n\text{-type: } \frac{1}{C^2} = \frac{2}{\varepsilon\varepsilon_0 e N_D}\left(E - E_{fb} - \frac{kT}{e}\right) \quad (3)$$

$$p\text{-type: } \frac{1}{C^2} = -\frac{2}{\varepsilon\varepsilon_0 e N_A}\left(E - E_{fb} - \frac{kT}{e}\right) \quad (4)$$

where C is the capacitance of space charge layer of the passive film, e is the elementary charge ($+e$ for electrons and $-e$ for holes), ε is the dielectric constant of the material under test, ε_0 the permittivity in vacuum (8.854×10^{-12} Fm^{-1}), N_D and N_A stand for the donor and acceptor electron density, E is the applied potential, and E_{fb}, the flat band potential, k the Boltzmann constant, T the absolute temperature. The donor or acceptor concentrations can be estimated from the slopes of the straight lines obtained. The Mott–Schottky's plot was obtained by performing a potential scan in the cathodic direction at 100 Hz in the potential range from +0.5 to −0.5 V around open circuit potential. A perturbing signal of 10 mV was used. E is the given potential, ε the dielectric constant of the coating, 'e' the electronic charge, and E_{fb} is the flat band potential.

The electronic property of double layer capacitor, associated with CMA Zn–Fe coatings may be explained using Mott–Schottky's equations, (3) and (4). The type of semiconductor can be determined from the C^{-2} vs. E plot. Figure 8 shows the C^{-2} vs. E profile for coating system, under optimized condition. A linear plot with positive slope indicated that protection efficacy of coatings is due to its n-type semiconductor (electrons are the charge carriers) nature.

Surface Morphology

Figure 9 shows the 2D deflection and 3D images of optimized Zn–Fe CMA coating. The mean roughness R_a and root-mean-square roughness Z_{rms} were determined based on AFM images using the SPIP™ software. The R_a value was 6.7 nm and the Z_{rms} value was 41.2. Formation of multiple layers of $(Zn–Fe)_{20}$ ($\sim$ 2.18 wt% Fe) and $(Zn–Fe)_{50}$ (4.99 wt% Fe) deposited at two different cathode current density was analyzed by SEM image. Cross-sectional view of CMA Zn–Fe coatings with 10 layers at optimized SCCDs of 20 and 50 mA cm^{-2} are shown in Fig. 10. Surface structure shows small granular structure, see Fig. 10(a). The discrete layers are observed in the cross-sectional view Fig. 10(b). Inspection of the microscopic appearance of the surface after corrosion tests was used to understand the reason for the improved corrosion resistance of the CMA coatings. The CMA coating was subjected to anodic polarization at +250 mV vs. OCP in 5% NaCl solution. The corroded

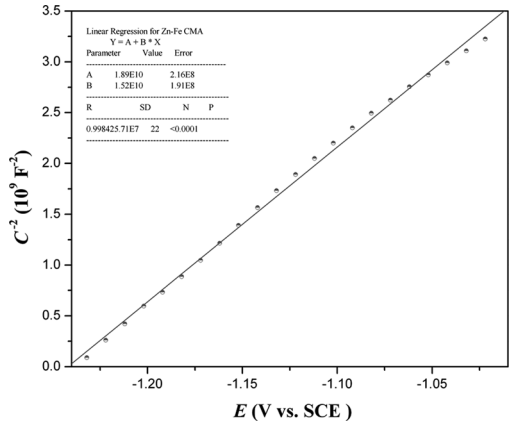

FIGURE 8.—Mott–Schottky plot of CMA $(Zn–Fe)_{20/50/120}$ coating system developed under optimal processing parameters.

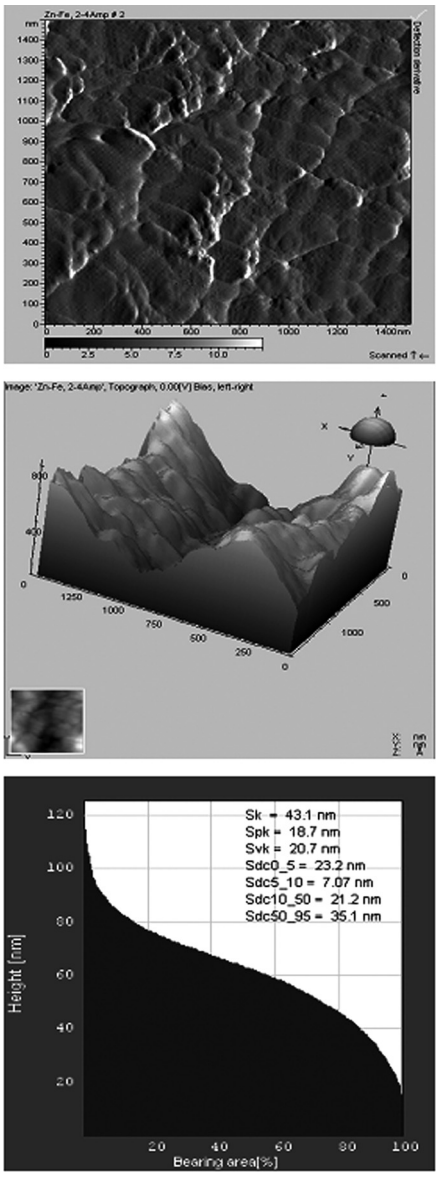

FIGURE 9.—Atomic force microscopic (AFM) image and surface roughness of CMA $(Zn–Fe)_{20/50}$ coating system with six layers.

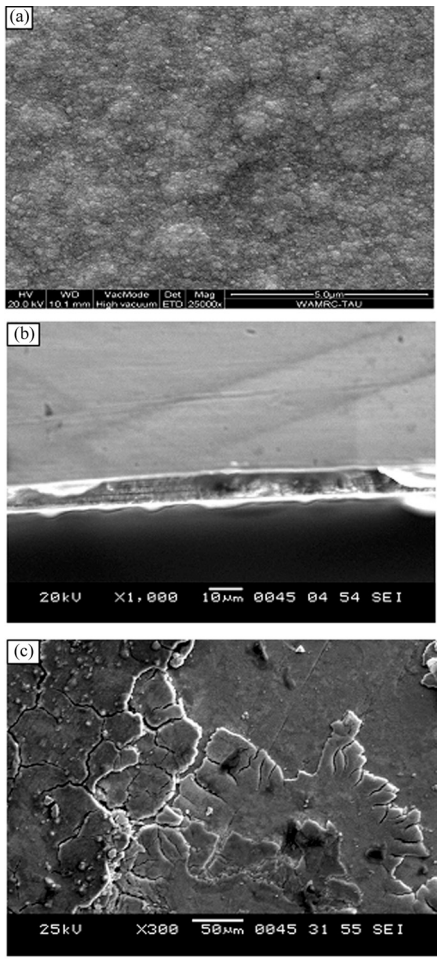

FIGURE 10.—SEM images of Zn–Fe CMA coating: (a) surface morphology; (b) cross-sectional view with different number of layers; and (c) surface after corrosion.

specimens were washed with distilled water and examined under SEM. Figure 10(c) shows a sample with CMA $(Zn–Fe)_{20/50/4}$ configuration, after corrosion test. The images in Fig. 10(c) show alternate layers alloys having different degree of cracks and crevices formed during process of deposition.

CONCLUSION

1. It is possible to develop a bright multilayered Zn–Fe alloy coating on to mild steel by single bath technique (SBT) using SA as brightener and AA as antioxidant.
2. The CMA (Zn–Fe) coating, having 120 layers deposited at 20 and 50 mA cm^{-2}, was found to show least corrosion rate (1.545×10^{-2} mmy^{-1}) compared to monolithic alloy of the same thickness (32.5×10^{-2} mmy^{-1}).
3. The electrodeposited CMA Zn–Fe alloy is about 20 times better corrosion resistant than monolithic Zn–Fe alloy of same thickness. However, it is less corrosion resistant than CMA Zn–Ni alloy coating.
4. The improved corrosion resistance of multilayer coatings is due to small change in the wt% Fe in alternate layers. The variation in deposition condition brings a significant change in the phase structure of alloys, which in turn lead to different types of scratches or crevices in alternate layers. Defects and failures occurring in a single layer in the deposition process are covered by the successively deposited coating layers. Therefore, the corrosive agent path is extended or blocked.
5. The high corrosion resistance of CMA Zn–Fe coatings is attributed to the dielectric barrier of the coatings, caused by decrease of relative dielectric constant ε_r of EDL capacitor on layering, supported by dielectric spectroscopy and Mott–Schottky's plot.
6. Corrosion resistance of CMA coating increased with number of layers, only up to a certain optimal level (120 layers) and then decreased. This may be attributed to less relaxation time for redistribution of metal ions (Zn^{+2}

and Fe^{+2}) at the diffusion layer, during deposition. In other words, at higher layer thickness, the CMA coating tends to become a monolithic.

Acknowledgments

The authors thank N. Eliaz from Materials and Nanotechnologies Program & School of Mechanical Engineering, Tel-Aviv University, Ramat-Aviv, Tel-Aviv 69978, Israel. We also thank Mario Levinstein from the Biomaterials and Corrosion Lab for his machinery and AFM work. And Zahava Barkay, Larisa Burstein, and Yuri Rosenberg from the Wolfson Applied Materials Research Center for their SEM/EDS analyses, respectively.

References

1. Wilcox, G.D.; Gabe, D.R. Electrodeposited zinc alloy coatings. Corrosion Science **1993**, *35*, 1251–1258.
2. Short, N.R.; Abibsi, A.; Dennis, J.K. Corrosion resistance of electroplated zinc alloy coatings. Trans. Inst. Met. Fin. **1984**, *67*, 73–77.
3. Roventi, G.; Fratesi, R. Normal and anomalous codeposition of Zn–Ni alloys from chloride bath. J. Appl. Electrochem. **2000**, *30*, 173–179.
4. Fei, J.-Y.; Wilcox, G.D. Electrodeposition of Zn–Co alloys with pulse containing reverse current. Electrochimica Acta **2005**, *50*, 2693–2698.
5. Gabe, D.R. Protective layered electrodeposits. Electrochimica Acta **1994**, *39*, 1115–1121.
6. Fei, J.-Y.; Liang, G.-Z.; Xin, W.-L. The structure and protective properties of zinc and nickel alternate electredeposits. Transactions of Materials and Heat Treatment **2005**, *25*, 1154–1158.
7. Xin, W.-L.; Fei, J.-Y.; Liang, G.-Z. Dual bath electrodeposition of alternate multilayer coatings of zinc and nickel deposits. Transactions of Materials and Heat Treatment **2005**, *25*, 1142–1145.
8. Ivanov, I.; Valkova, T.; Kirilova, I. Corrosion resistance of compositionally modulated Zn–Ni multilayers electrodeposited from dual baths. J. Appl. Electrochem. **2002**, *32*, 85–89.
9. Kirilova, I.; Ivanov, I.; Rashkov, St. Anodic behaviour of compositionally modulated Zn–Co multilayer eletrodeposited from single and dual baths. J. Appl. Electrochem. **1998**, *28*, 1359–1363.
10. Fei, J.-Y.; Liang, G.-Z.; Xin, W.-L.; Wang, W.-K. Surface modification with zinc and Zn–Ni Alloy compositionally modulated multilayer coatings. Journal of Iron and Steel Research International **2006**, *13* (4), 61–67.
11. Fei, J.-Y.; Liang, G.-Z.; Xin, W.-L.; Liu, J.-H. Corrosion performance of Zinc and Zinc-cobalt alloy compositionally modulated multilayer (CMM) coatings. Journal of Wuhan University of Technology – Mater. Sci. Ed. **2006**, *21* (4), 40–44.
12. Wilcox, G.D. Surface modification with compositionally modulated multilayer coatings. Journal of Corrosion Science and Engineering **2004**, *6*, 52.
13. Thangaraj, V.; Eliaz, N.; Chitharanjan Hegde, A. Corrosion behavior of composition modulated multilayer Zn–Co electrodeposits produced using a single-bath technique. J. Appl. Electrochem. **2009**, *39* (3), 339–345.
14. Ekerm, A.; Fatih, U. Correlation between sputtering conditions and growth properties of (TiAl)N/AlN multilayer coatings. Materials and Manufacturing Processes **2009**, *24*, 796–799.
15. Kamachi Mudali, U.; Khatak, H.S.; Baldev Raj; Uhlemann, M. Surface alloying of nitrogen to improve corrosion resistance of steels and stainless steels. Materials and Manuracturing process **2004**, *19*, 61–73.
16. Prabhu Ganesan; Swaminatha Kumaraguru, P.; Branko Popov, N. Development of compositionally modulated multilayer Zn–Ni deposits as replacement for cadmium. Surface & Coatings Technology **2007**, *201*, 7896–7904.
17. Nasser Kanani. *Electroplating: Basic Principles, Processes and Practice*; Elsevier Ltd.: Berlin, Germany, 2006.
18. Gellings, P.J.; Bouwmeester, H.J.M. *Handbook of Solid State Electrochemistry*; CRC Press: Netherlands, 1997.
19. Yuan, X.; Song, C.; Wang, H.; Zhang, J. *Electrochemical Impedance Spectroscopy in PEM Fuel Cells – Fundamentals and Applications*; Springer Publications: London, 2010.
20. Ravinder, D.; Latha, K. Dielectric behavior of mixed Mg–Zn ferrites at low frequencies. Mater. Lett. **1999**, *41*, 247–253.
21. Morison, S.R. *Electrochemistry at Semiconductor and Oxidized Metal Electrodes*; Plenum Press: New York, 1980; 49.